Building and Environment 169 (2020) 106591

Contents lists available at ScienceDirect

Building and Environment

journal homepage: http://www.elsevier.com/locate/buildenv

A relationship for the diffusion coefficient in eddy diffusion based indoor dispersion modelling

Timothy Foat [a,b,*], Joseph Drodge [a], James Nally [a], Simon Parker [a]

[a] Dstl, Porton Down, Salisbury, Wiltshire, SP4 0JQ, UK
[b] Faculty of Engineering and Physical Sciences, University of Southampton, Hampshire, SO17 1BJ, UK

ARTICLE INFO

Keywords:
Eddy diffusion
Indoor dispersion
Exposure
CFD
Vapour detection
Explosives

ABSTRACT

Turbulent or eddy diffusion models are used to predict spatially resolved exposures to toxic airborne materials in indoor environments. The single parameter that governs mixing in these models is the eddy diffusion coefficient. Some relationships that enable this coefficient to be predicted have been proposed in the literature, but wider applicability of these has not previously been tested. In this paper an automated computational fluid dynamics tool was used to calculate the eddy diffusion coefficient in a range of isothermal, mechanically ventilated rooms. Available models for the diffusion coefficient were then tested and the most applicable was found to be one based on a turbulent kinetic energy balance. This relationship was only appropriate when the characteristic length was set to a dimension of the air supply inlet, instead of the length usually applied, i.e. the room height. The validity of this relationship was further demonstrated using experimental test cases and by applying standard error metrics. The eddy diffusion approach can now be used with improved confidence in a wider range of scenarios than was possible before.

1. Introduction

Mathematical models are used to calculate the exposure of individuals to airborne toxic material in indoor environments [1]. The models need to be simple when it is not practical to fully survey the environment. In such cases it may not be possible to define the boundary conditions required for more complex techniques such as computational fluid dynamics (CFD) modelling. Another significant advantage of most simple models is the speed with which they can be set up and solved. This means that they can be used when limited time is available.

A number of simple modelling techniques are available for predicting the hazard from airborne material in single rooms indoors, these include: well-mixed zone models [2], two-box or two-zone models [3], dilution ventilation and mixing factor models [4], zonal models [5], Markov chain models [6] and eddy diffusion models [7–10]. It should be noted that CFD models can also be solved rapidly using techniques such as those employed in the fast fluid dynamics method [11,12] and the lattice Boltzmann method [13,14]. However, detailed information about the indoor space is still required for these models.

Eddy diffusion models for indoor spaces work by solving a three dimension analytical diffusion model which can account for containment of the transported material by the walls of the room. The containment effect is incorporated through the use of image sources [15]. When the room is large or transport times are short, it is not always necessary to include the effect of the walls. Eddy diffusion models have an advantage over the other simple modelling techniques mentioned above, with the exception of zonal models, in that they provide a representation of the spatially resolved concentration field.

Eddy diffusion models are used to predict spatially resolved exposures to toxic airborne materials in indoor environments, for example see Refs. [16–19]. The method is also described in the American Industrial Hygiene Association (AIHA) book 'Mathematical Models for Estimating Occupational Exposure to Chemicals' [7] and is one of the tools included in the AIHA IH Mod 2.0 software [20].

Eddy diffusion models could have application in areas other than the prediction of exposure, such as transport of vapour from explosives for detection purposes [21]. For example, training scenarios are often created where explosives are placed in a room and detection dogs are brought into the space to see whether they can find the concealed material. Rapid running dispersion models could be used to provide insight into how the vapour concentration varies throughout the day.

Different formulations of the eddy diffusion equations are available

* Corresponding author. Dstl, Porton Down, Salisbury, Wiltshire, SP4 0JQ, UK.
E-mail addresses: tgfoat@dstl.gov.uk (T. Foat), jdrodge1@dstl.gov.uk (J. Drodge), jnally@dstl.gov.uk (J. Nally), stparker@dstl.gov.uk (S. Parker).

https://doi.org/10.1016/j.buildenv.2019.106591
Received 12 July 2019; Received in revised form 29 November 2019; Accepted 9 December 2019
Available online 13 December 2019

depending on the type of source term applied. For an instantaneous point source the variation in concentration, C, in space and time is given by the following [9]. It should be noted that all units in this paper are SI unless otherwise stated.

$$C(x,y,z,t) = \frac{M \exp(-\lambda_f t)}{8(\pi K t)^{\frac{3}{2}}} r_x r_y r_z, \quad (1)$$

where M is the mass of material released at time $t = 0$ at a point in space and x, y and z are the Cartesian coordinates at which C is calculated. λ_f is the fresh air change rate and K is the eddy diffusion coefficient, which governs the rate of mixing. The wall reflection terms, r_x, r_y and r_z, are given by the following [9]:

$$r_x = \sum_{n=-\infty}^{\infty} \left[\exp\left(\frac{-(x + 2nL - x_0)^2}{4K t} \right) + \exp\left(\frac{-(x + 2nL + x_0)^2}{4K t} \right) \right], \quad (2)$$

$$r_y = \sum_{n=-\infty}^{\infty} \left[\exp\left(\frac{-(y + 2nW - y_0)^2}{4K t} \right) + \exp\left(\frac{-(y + 2nW + y_0)^2}{4K t} \right) \right], \quad (3)$$

$$r_z = \sum_{n=-\infty}^{\infty} \left[\exp\left(\frac{-(z + 2nH - z_0)^2}{4K t} \right) + \exp\left(\frac{-(z + 2nH + z_0)^2}{4K t} \right) \right], \quad (4)$$

where x_0, y_0 and z_0 are the release coordinates, L, W and H are the length, width and height of the room and the summation is over the image sources. As can be seen, x, y and z correspond with L, W and H respectively. Rather than an infinite sum, only a small number of images sources are required to give a sufficiently accurate solution when the non-dimensional diffusion time, t_{ND}, is small. t_{ND} is defined as ($t\,K/\,L_{diff}^2$) where L_{diff} is the distance over which the material is diffusing e.g. the length of the room. Cheng et al. [10] used six images sources and Nehorai [8] used only one.

The eddy diffusion coefficient for indoor spaces has been calculated from a number of experimental studies [7,9,10,16,22,23] and empirical or *a priori* relationships have been produced for certain situations [9,10,24]. The experimentally calculated values have been shown to range from a lower limit of 1×10^{-3} m s^{-2} [9] to as high as 1.9×10^{-1} m s^{-2} [7]. Which makes it difficult to directly apply the experimentally derived diffusion coefficients to cases were K is not known.

The Karlsson et al. relationship [24] is based on a turbulent kinetic energy balance (TKEB) and the assumption that the total rate of change of the turbulent kinetic energy in the system is zero. This relationship can be simplified to Equation (5) for isothermal rooms [9]. In Equation (5) the first term is the mechanical production of turbulent kinetic energy and the second is the dissipation.

$$\frac{\lambda u_0^2}{2} - \frac{c_\varepsilon u_{turb}^3}{L_{char}} = 0, \quad (5)$$

where λ is the total air change rate, u_0 is the velocity at the inlet, c_ε is a constant and u_{turb} is a representative turbulent velocity. The dissipation term is typically thought to apply in high Reynolds number flows with L_{char} referring to the integral length scale, the size of the largest eddies in the flow. Karlsson et al. gave $c_\varepsilon = 0.032$. Using Equation (6), which gives a relationship between K, u_{turb} and L_{char} (also typically referring to the integral length scale), an equation for K (Equation (7)), as a function of measurable parameters, can be derived [9,24].

$$K = c_\nu u_{turb} L_{char}, \quad (6)$$

$$K = \sqrt[3]{\frac{\lambda u_0^2 c_\nu^3 L_{char}^4}{2 c_\varepsilon}}, \quad (7)$$

where c_ν is the von Karman constant ($c_\nu = 0.4$ has been used here). Drivas et al. [9] did not give Equation (7) directly and they also assumed that both c_ν and c_ε were equal to 0.4 (without providing a rationale). Drivas et al. [9] and Shao et al. [23] assumed that L_{char} was equal to H, which, it will be proposed in this paper, should not be the case.

Cheng et al. [10] reported an empirical relationship for K (Equation (8)) based on experimental data from two naturally ventilated residential rooms with air change rates of up to 5.4 h^{-1}.

$$\frac{K}{V^{2/3}} = 0.52\lambda + 8.61 \times 10^{-5} \frac{1}{\text{s}}, \quad (8)$$

where V is the room volume.

Cheng et al. [10] also considered that K might be related to λ alone, but this approach resulted in a room specific relationship for K.

Shao et al. [23] demonstrated the validity of the TKEB relationship [9] up to an air change rate of 2.9 h^{-1} for a single bespoke test chamber when they set L_{char} to the room height.

Even with the above studies there is limited data on how the eddy diffusion coefficient varies in a range of rooms [25].

The aim of the present work was to use CFD to calculate K in a large number of rooms and to compare these calculated values to those from the relationships discussed previously. This was done in order to determine which, if any, of the relationships are valid over a wide range of room sizes and ventilation conditions.

2. Methodology

2.1. Overview

An automated CFD method described by Foat et al. [26] was used to produce models for scalar transport from an instantaneous release in approximately 250 different isothermal, mechanically ventilated rooms. The eddy diffusion model given in Equation (1) was then fitted to the CFD scalar concentration predictions to give a value of K for each room. The relationship between the eddy diffusion coefficient and the room geometry and ventilation parameters was then compared to the existing relationships given in the introduction.

Before running the automated CFD study the modelling method was validated against an experimental test case.

2.2. CFD validation

The validation experiment was conducted in a cuboid shaped meeting room which was 13.0 m long, 7.0 m wide and 2.6 m high with a small cut out in one corner. The room volume was 237 m^3, the floor aspect ratio was 1.9 and H/(floor area)$^{1/2}$ = 0.27. The room had mixing ventilation with the air supplied through eight diffusers and extracted through four, which were all located on the ceiling. All ceiling diffusers were square, four-way diffusers (effective air discharge area of each diffuser, $A = 0.0446$ m^2). In the model, the effective air discharge area for the inlet was used, as opposed to the open area to ensure that the correct momentum was applied [27]. Also in the model, the air was set to enter the room with an angle of 30° to the horizontal. In the experiment, the total air flow rate was 1.0 m^3 s^{-1} and the recirculation fraction was 0.56, giving a fresh air change rate of 6.8 h^{-1} and total air change rate, λ, of 15.4 h^{-1}.

A tracer gas, propylene, was released in the corner of the room (1 m high and 1 m from each wall) through a spherical diffuser (a device designed to reduce the momentum of a jet of gas). A cylinder of 2% propylene in nitrogen was used to deliver 0.04 m^3 of the tracer at an approximately constant rate over a period of 180 s. The gas concentration was monitored in the test room using seven Ultra-Violet Ion Collectors (UVICs), Mk II, photo-ionisation detectors [28]. Six of the UVICs were positioned 0.65 m above the ground with one at 1.95 m height. Fig. 1 shows the meeting room and the layout used in the experiment.

IconCFD® version 3.3.9 (ICON®, United Kingdom) was used to produce a cut-cell mesh for the room (iconHexMesh [29]) and to solve the flow and scalar transport (iconSimpleFoam and iconSpeciesFoam

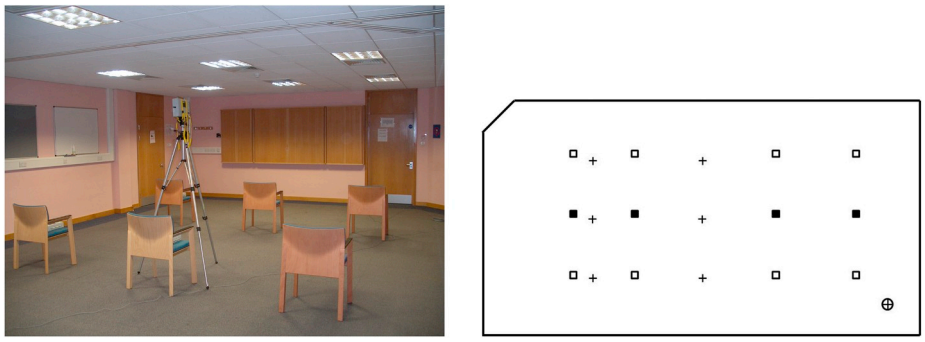

Fig. 1. The meeting room used for the validation experiment. The photograph show the chairs on which the UVICs were placed and the UVIC at 1.95 m height. The schematic shows a plan view of the layout used in the experiment. The open squares indicate the supply vents, the filled squares the extract vents, the crosses indicate the UVIC locations and the circle with a cross shows the tracer gas release location.

[29]). The IconCFD software is an open source based CFD product which makes use of openFOAM® technology. It was assumed that the flow was steady and turbulent. The supply diffusers were given fixed volume flow rates and the extracts were pressure outlets. All walls were given no-slip boundary conditions. The flow field was solved for 7000 iterations to produce a converged solution. The scalar transport was then solved transiently using the steady-state flow solution. The k-ω SST turbulence model was used and the turbulent Schmidt number, Sc_t, was set to 0.7. The SIMPLE scheme [30] was used for the pressure-velocity coupling, a second-order MUSCL scheme [31] was used for the momentum transport terms and a first-order upwind scheme was used for all scalar terms. A first-order implicit scheme was used for the transient scalar transport.

The validation model had a base mesh (refinement level zero) of 0.1 m with the mesh on the supply and extract vents at refinement levels three and two respectively. The mesh on the wall, ceiling and floor was at refinement level one. The non-dimensional distance from the wall of the first cell centre, y_1^+, was less than 500 on all walls apart from in the fast flowing air leaving the inlets. The size of the mesh is within the limits for coarse CFD as defined by Wang and Zhai [32]. The mesh on a vertical plane through an extract and two supplies is shown in Fig. 2. The time step size, Δt, was 1.0 s. The method used to assess the performance of the models is given below. The model was tested for mesh and time step sensitivity. Model sensitivities (to mesh size, Δt and Sc_t) were also considered as part of the automated CFD study (Section 2.6).

Predictions from the model were compared to data at each of the seven UVIC locations and quality metrics were calculated (see below). The minimum, average and maximum concentrations for all the locations at each time are shown in Fig. 3. It should be noted that the comparison shown in the graph does not directly compare the concentration at one location in the CFD model with the same location in the experiment but represents some statistical characteristics of the concentration field. However, model performance metrics were calculated by comparing data at each corresponding location.

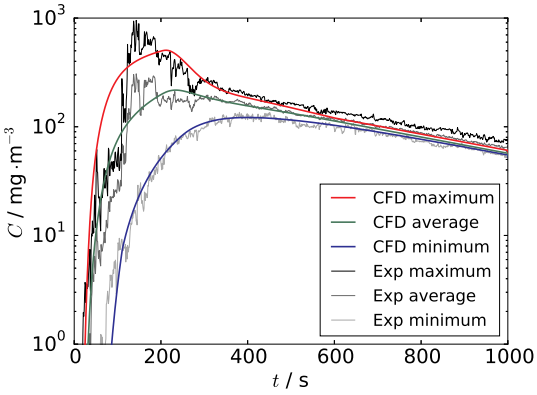

Fig. 3. Maximum, average and minimum tracer concentrations across seven measurement locations from two experiments compared to predictions from the CFD model.

The CFD does not capture some of the unsteadiness in the concentration field, as would be expected when using a steady Reynolds averaged Navier-Stokes modelling approach. However, the model captures the trends well.

The model performance was assessed by calculating the geometric mean bias (MG) and geometric variance (VG), as defined by Ref. [33]. Data points were included in the assessment when the measured concentration was greater than 1 mg m^{-3}. This was approximately the lowest concentration at which the UVICs were calibrated. The ideal value for both metrics is 1. MG, which indicates the bias, was 0.95, therefore the model only slightly over-predicted the experiment (by a factor of 1.05, based on the geometric means). VG, which indicates the

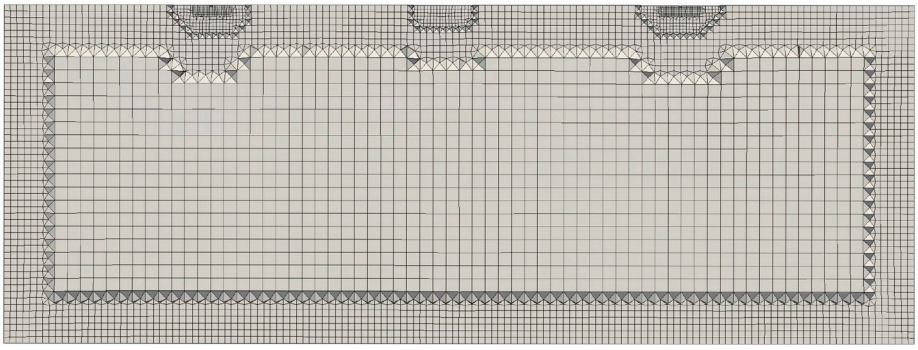

Fig. 2. The mesh used for the meeting room model shown on a vertical plane through two supply vents and an extract vent. The extract is shown in the middle of the image with supply vents either side.

scatter, was 1.01, therefore the model data was similarly distributed to the experimental data.

2.3. Scenario for the automated CFD study

The approximately 250 isothermal, mechanically ventilated rooms modelled were all cuboid in shape and contained no furniture. They were served by mixing ventilation with no recirculation, via supply and extract vents (square four-way diffuser) located in the ceiling. The room volume and shape, the air change rate and vent layout were varied across the parameter space shown in Table 1. Six example room layouts are shown in Fig. 4. It should be noted that the rooms studied consisted of only a small subset of possible indoor environments.

The automated CFD method used a Sobol sequence experimental design [34] to produce models which effectively covered the range of the parameters give in Table 1. The rationale for these ranges is given in Foat et al. [26].

Supply grilles were based on Trox ADT 4-way diffusers [35]. A diffuser with an effective air discharge area, A, of 0.012 m^2, designed for a flow rate of 0.03 $m^3\ s^{-1}$, was chosen for rooms with a total flow rate up to 0.3 $m^3\ s^{-1}$, limiting the number of small diffusers in the room to ten. A diffuser with $A = 0.045\ m^2$, designed for a flow rate of 0.16 $m^3\ s^{-1}$, was chosen for rooms with a total flow rate between 0.3 $m^3\ s^{-1}$ and 1.6 $m^3\ s^{-1}$. A diffuser with $A = 0.112\ m^2$ was specified for rooms with higher flow rates. The number of supply vents in the room was calculated based on the throw and guidance given in Awbi [36] which states that "the throw should ideally be equal to the distance from a wall or half the distance to the next adjacent diffuser".

Three sizes of extract grille were used: $(0.4\ m)^2$ and $(0.6\ m)^2$ and 0.6 m × 1.2 m. The smallest grilles were used for total room flow rates less than 5 $m^3\ s^{-1}$, the middle size was specified for flow rates between 5 $m^3\ s^{-1}$ and 10 $m^3\ s^{-1}$ and the largest size for flows above 10 $m^3\ s^{-1}$. The number of vents was chosen so that the mean velocity through the grille was approximately 4 m s^{-1} [37]. The spacing of supply diffusers and extract grilles was the same as used in Ref. [26].

The scenario modelled was an instantaneous release of material from one of three locations: the centre of the room (centred in length, width and height), one corner of the room (1 m in from both walls and centred in height), mid-point (mid-way between the centre of the room and one corner and centred in height).

2.4. Automated CFD method

Salome V6.5.0 (Open Cascade, France), an open source integration platform for numerical simulation, was used to generate the STL surfaces of the geometries. IconCFD version 3.3.9 (ICON, United Kingdom) was used for the meshing (iconHexMesh [29]) and the CFD solutions (iconSimpleFoam and iconSpeciesFoam [29]). The automated CFD used the same model settings and meshing approach as applied in the validation modelling (see Section 2.2). This included a second-order MUSCL scheme for the momentum transport terms, a first-order upwind scheme for all scalar terms and a first-order implicit scheme for the transient scalar transport. The first-order schemes were chosen as these had been shown to give accurate results in the validation modelling and to improve convergence in the automated study.

Table 1
Experimental design space. The number of points within each range was determined by Sobol sequence experimental design [34].

Parameters	Symbol	Ranges
Room volume	V	50 m^3–5000 m^3
Floor aspect ratio	L/W	1–3
Height/(floor area)$^{1/2}$	$H/(LW)^{1/2}$	0.1–1.5
Air change rate	λ	0.5 h^{-1} - 20 h^{-1}
Release location		Centre, corner or mid-point

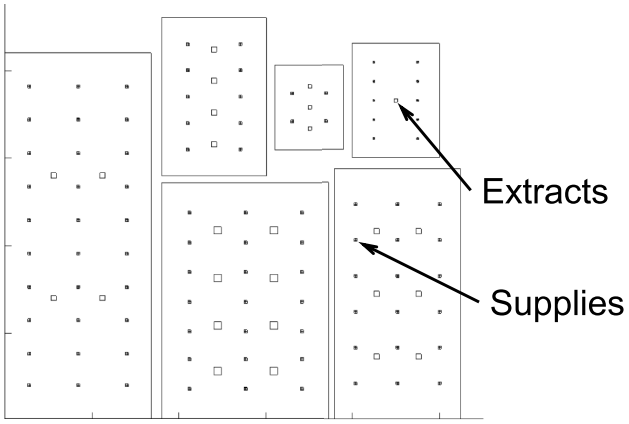

Fig. 4. Plan views of six example rooms showing the supply and extract vent layouts. The supply vents are shaded, the extracts are open squares. The tick marks on the axes are spaced at 10 m intervals.

2.5. Fitting the eddy diffusion model to the CFD data

The eddy diffusion model, Equation (1) (with five image sources), was fitted to the CFD data by minimising the geometric variance (VG), to a value of 1, by varying K.

For each CFD model the optimum eddy diffusion coefficient was calculated independently over three planes at heights of 0.5 m, 1.0 m and 1.5 m. These planes were chosen to cover the occupied zone. On each plane, data from 20 locations was used at times with 10 s intervals up to 1500 s after the start of the release. It was confirmed that the results did not change significantly with an increase in the number of locations used or a decrease in the size of the time intervals. Any location within 2 m of the release location was not included, as close to the source the concentration field was more strongly affected by local flow features. Any data point with a concentration below 1×10^{-20} kg m^{-3} was excluded to avoid the VG calculations being skewed by large differences between the CFD and eddy diffusion models at these very low values. A single VG value was calculated for each plane for each CFD model i.e. it incorporated equally weighted data from all locations on that plane and all time points.

The model fitting was performed using a Python script, the SciPy optimize. minimize function and the L-BFGS-B algorithm [38].

A subset of the automated models were used to test the sensitivity of the K calculations to the mesh, time step and Schmidt number.

The input data from the automated CFD study together with the K values for the fitted eddy diffusion model are given in the supplementary material.

2.6. Mesh, time step and turbulent Schmidt number sensitivity

A subset (10) of the 250 CFD models were re-run with three different base mesh sizes (0.079 m, 0.100 m, 0.126 m), three Δt values (0.5 s, 1.0 s, 2.0 s) and three Sc_t value (0.5, 0.7, 0.9) with K calculated for each model. The geometric mean bias (MB) was calculated for the predicted K for each parameter change, with the original model as a reference. The results of the sensitivity study are given in Table 2.

With a base mesh size of 0.1 m the MB for K with $\Delta t = 2.0$ s compared to $\Delta t = 1.0$ s was 1.06, i.e. the geometric mean K for $\Delta t = 1.0$ s was 106% of that for $\Delta t = 2.0$ s. For $\Delta t = 0.5$ s compared to $\Delta t = 1.0$ s, MB was 1.24, i.e. the geometric mean K for $\Delta t = 1.0$ s was 124% of that for $\Delta t = 0.5$ s. Therefore, the results did show some time step dependence but due to the spread in the calculated K values (almost two orders of magnitude) and the quality of the validation shown previously (where

Table 2
Results of the CFD model sensitivity test.

Fixed parameters	Compared parameters	MB
Sc_t = 0.7, Mesh = 0.1 m	Δt = 2.0 s vs. 1.0 s	1.06
	Δt = 0.5 s vs. 1.0 s	1.24
Sc_t = 0.7, Δt = 1.0 s	Mesh = 0.126 m vs 0.100 m	1.11
	Mesh = 0.079 m vs. 0.100 m	1.02
Δt = 1.0 s, Mesh = 0.1 m,	Sc_t = 0.9 vs. 0.7	1.07
	Sc_t = 0.5 vs. 0.7	0.94

Δt of 1.0 s was used), a Δt of 1.0 s was deemed acceptable for the automated study. There was also mesh size dependence but this was small between the 0.1 m and 0.079 m meshes. Therefore, the 0.1 m base mesh was deemed acceptable for the automated study. The geometric mean K decreased as Sc_t increased, as would be expected. A range of values for Sc_t has been used in different studies, such as 0.2 to 1.3 reported by Tominaga et al. [39]. However, Sc_t = 0.7 has been widely applied [40] and was used successfully in the validation exercise, therefore, this was deemed the most suitable value for the automated study.

3. Results and discussion

The results from fitting the eddy diffusion model to the automated CFD data are given below. Initially only data for the centre release location is shown. Fig. 5 shows four possible methods for predicting the eddy diffusion coefficient. The four methods are: a simple correlation of K with the air change rate, the Cheng et al. [10] empirical relationship (Equation (8)) and the TKEB relationship (Equation (7)) with two different definitions of the characteristic length, L_{char}. For each method a linear regression line, with an intercept of zero, has been fitted. The equation of the regression line and the coefficient of determination, R^2, value are also shown. R^2 was calculated according to Eisenhauer [41].

As shown in Section 1 the characteristic length scale, L_{char}, in the TKEB relationship is used in both the dissipation rate term in Equation (5) and in Equation (6). In both cases it usually refers to the integral length scale. The integral length scale in a room could be a function of the dimensions of the inlet and the jet of air produced there, or the dimensions of the room. If L_{char} was related to H then, according to Equation (7), taller rooms will tend to have higher values of K which seems counter-intuitive. In a taller room more of the mixing energy introduced at ceiling mounted inlets would have been dissipated by the time the air reaches the occupied zone. Therefore, it is proposed here that it should be related to the inlet when being used to calculate the eddy diffusion coefficient. To assess which is the best definition for L_{char}, results have been plotted for the TKEB relationship with L_{char} equal to the room height or the square root of the inlet area, A.

If L_{char} is set to the square root of A, then Equation (7) can be simplified to Equation (9).

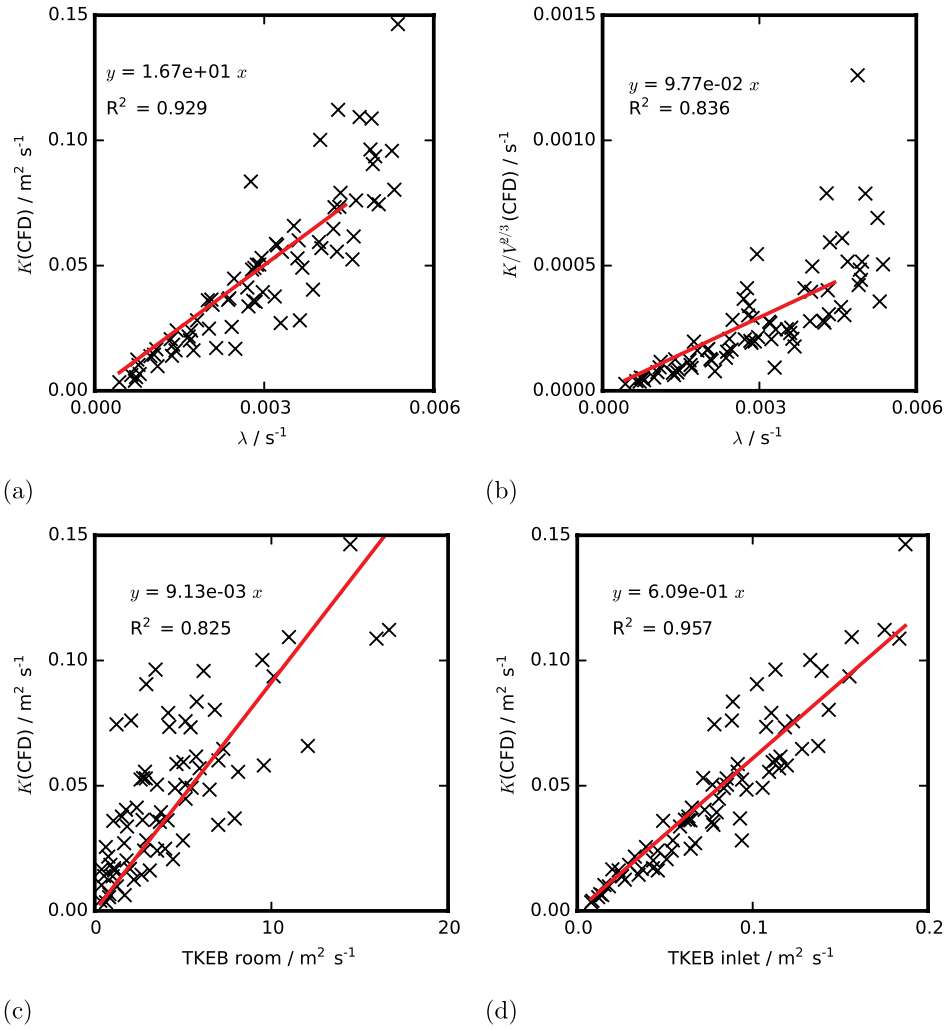

Fig. 5. K or $K/V^{2/3}$, calculated by fitting an eddy diffusion model to the CFD data, plotted against four possible methods: (a) the ACR, (b) the Cheng et al. relationship (Equation (8)), (c) the TKEB relationship (Equation (7)) with L_{char} = H and (d) the TKEB relationship (Equation (7)) with L_{char} = $\sqrt{A}$. The red line shows the linear regression line. Only data for the releases in the centre of the room is shown here. (For interpretation of the references to colour in this figure legend, the reader is referred to the Web version of this article.)

$$K = c\frac{Q}{\sqrt[3]{V N^2}}, \tag{9}$$

where c is a constant which equals $(c_v\sqrt[3]{1/2c_\varepsilon})$, Q is the total volume flow rate into the room and N is the number of supply vents. For the values of c_v and c_ε used in this paper, $c = 1$.

From the results shown in Fig. 5, the best method for calculating K, based on R^2, is the TKEB relationship with the characteristic length set to $\sqrt{A}$, where $R^2 = 0.957$. The TKEB relationship with $L_{char} = H$ performs significantly worse with an R^2 of 0.825. The gradient of the line for the TKEB relationship with $L_{char} = H$ is small (9.1×10^{-3} compared to 6.1×10^{-1} for $L_{char} = \sqrt{A}$) which means that K values calculated using this relationship would be higher than those measured. Shao et al. [23] used the TKEB relationship with $L_{char} = H$ and got only a small over-prediction compared to their experimental data. The small difference is possibly due to the low height of their room (2 m) and relatively large effective inlet area (0.232 m^2).

The Cheng et al. [10] relationship shows a small R^2 value (0.836), meaning that their relationship does not apply well to this data set. However, the rooms examined by Cheng et al. were naturally ventilated through open windows, whereas the rooms modelled here were mechanically ventilated with ceiling located supply and extract.

The air change rate relationship performs reasonably well with $R^2 = 0.929$, but there is a large spread of data at higher air change rates. A spread of the same extend is not present with the TKEB $\sqrt{A}$ relationship.

3.1. Effect of release location and plane height

As stated previously, K was calculated by fitting the eddy diffusion model (Equation (1)) independently over three planes at heights of 0.5 m, 1.0 m and 1.5 m. The geometric mean bias (MB) was calculated between the data for the planes at 1.5 m and 1.0 m and for the planes at 0.5 m and 1.0 m. For the planes at 1.5 m and 1.0 m, the MB was 1.00. For the planes at 0.5 m and 1.0 m, the MB was 0.95. Therefore, there was only a small decrease in K nearer to the floor.

The data from the three release locations: centre, mid-point and corner, is shown in Fig. 6. The steepest gradient of the linear regression line is for the releases in the corner of the room (1.15) and the shallowest is for releases in the centre of the room (0.61). The gradient for releases at the mid-point is slightly larger than that for centre releases. The CFD derived diffusion coefficients for the corner releases compared to other release locations are most likely higher due to the type of ventilation used in the rooms. The square four-way diffusers on the ceiling produce jets which attach to the ceiling and then move down adjacent walls. Jets can also be forced downward where jets from two adjacent diffusers meet [26]. This means that air flow close to walls or inter-diffuser boundaries (at the horizontal planes considered here) should be faster than flows at other locations. As the corner releases are always located close to a wall then they should always experience the higher air flow from the diffuser jet. It is assumed that the faster mixing for corner releases is caused by this effect.

3.2. All data combined

CFD derived diffusion coefficients for every release location are plotted in Fig. 7 along with the linear regression line, 95% confidence intervals (CI) and 95% prediction intervals (PI). The equation for the regression line is also shown.

The equation for the linear regression line, which describes the TKEB relationship using $\sqrt{A}$ as the characteristic length, is given below. Straight line approximations to the upper and lower PI lines are also given.

$$K(\text{upper PI}) = 0.827\frac{Q}{\sqrt[3]{V N^2}} + 0.0565\ \frac{m^2}{s}, \tag{10}$$

$$K(\text{regression}) = 0.824\frac{Q}{\sqrt[3]{V N^2}}, \tag{11}$$

$$K(\text{lower PI}) = 0.822\frac{Q}{\sqrt[3]{V N^2}} - 0.0565\ \frac{m^2}{s}. \tag{12}$$

The linear regression line equation shows that, based on the CFD data used here, a constant equal to 0.824 should be applied to the simplified TKEB relationship given in Equation (9). It is proposed that Equation (11) can be used to calculate K for use in an eddy diffusion

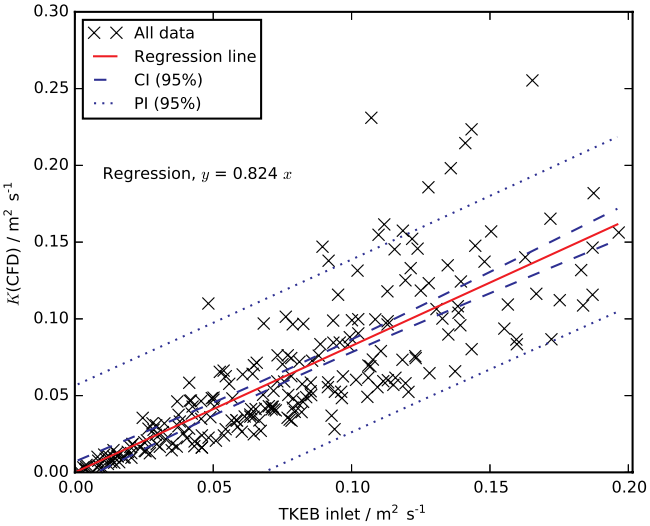

Fig. 7. K, calculated from the CFD, plotted against the TKEB relationship, using Equation (9), for all release locations.

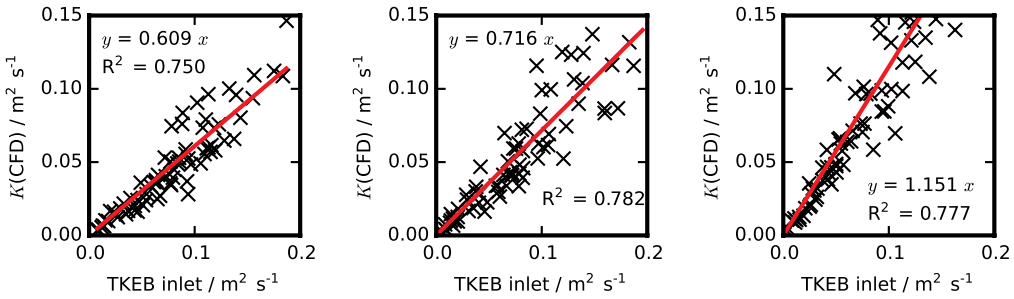

Fig. 6. K, calculated from the CFD, plotted against the TKEB relationship, using Equation (9), for the three release locations: centre (left), mid-point (middle) and corner (right). The red line shows the linear regression line. (For interpretation of the references to colour in this figure legend, the reader is referred to the Web version of this article.)

model when only Q, V and N are known. Due to the spread of CFD derived diffusion coefficients around the regression line, Equations (10) and (12) can be used to calculate a possible range of value for K. As it has been suggested [9] that the lower limit for K is 0.001 m^2s^{-1}, this bound should be applied when using these equation. In Section 3.3 the validity of using this approach is demonstrated through comparisons with experimental data.

To understand the error between the fitted eddy diffusion model and the CFD predictions, VG is plotted against K in Fig. 8 for the plane at 1 m.

Fig. 8 shows that VG can be large, so the concentrations predicted by the fitted diffusion model can be widely scattered around the CFD data. This scatter increases as K decreases. For $K < 0.01$ m^2s^{-1}, VG is greater than 1000 in most cases. A VG of 1000 indicates a factor of 14 scatter. For $K > 0.05$ m^2s^{-1}, VG is less than 100 (indicating a factor of nine scatter) in 79% of cases and less than 10 in 46% of cases.

It should be noted that eddy diffusion models can be less accurate close to the source when the non-dimensional diffusion time, t_{ND}, is small (L_{diff} here is the distance from the source). Close to the source the concentration field will be more affected by local flow features, which eddy diffusion models are not designed to predict. When t_{ND} is small, a small error in the model can have a large effect on the concentration. The poor model performance when t_{ND} is small explains why VG tends to increase as K decreases in Fig. 8 (all models were run for 1500 s). Running the models that have smaller values of K (e.g. models with low air change rates) for longer should reduce VG.

3.3. Comparison with experimental data

The TKEB relationship using $\sqrt{A}$ as the characteristic length has been compared to experimental data using two methods. Firstly, the experimentally derived eddy diffusion coefficients of Cheng et al. [10] and Shao et al. [23] have been compared to the CFD derived coefficients and the TKEB relationship. Secondly, an eddy diffusion model, with K calculated using the TKEB relationship, has been used to predict gas concentrations in two scenarios and results have been compared to experimental data.

3.3.1. Comparison with experimentally derived eddy diffusion coefficients

Cheng et al. [10] conducted indoor dispersion experiments in two naturally ventilated residential rooms. They used a continuous gas release, measured concentrations at 30 or 37 locations and then averaged concentrations both temporally and radially. Ventilation of the building was via windows, which were opened by different amounts for each experiment. Shao et al. [23] conducted a number of experiments in a bespoke test chamber. They used a continuous gas release and measured concentrations at two locations. The air was supplied to their room via a filter bank onto which four air diffusers were fitted. From both of these sets of experiments the authors calculated eddy diffusion coefficients.

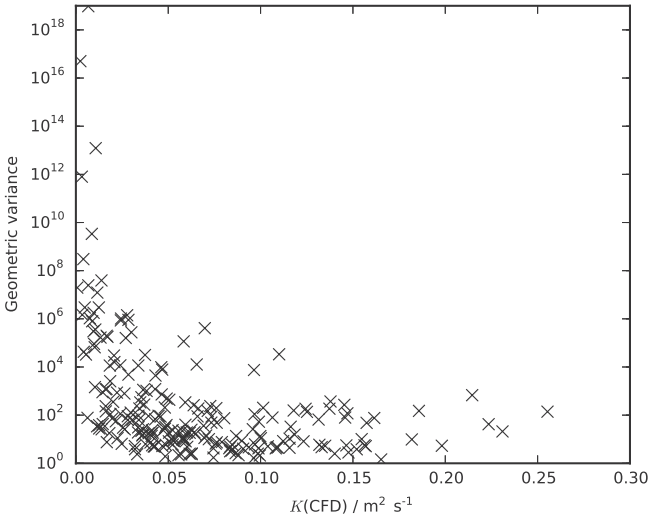

Fig. 8. VG between each fitted diffusion model and the CFD concentration data.

In order to compare the data of Cheng et al. [10] and Shao et al. [23] to the TKEB relationship (Equation (11)), Q, V and N are required. In both cases Q was calculated from the provided values for λ and V. V was used as provided, however, it is possible that a larger value for V could have been used with the Cheng et al. data as more than just a single room was being ventilated. N was set to 1 for the Shao et al. data and to 2 for the Cheng et al. data. In the Cheng et al. experiments, three windows were open, but it was assumed here that one of these was acting as an outflow. Therefore, there is uncertainty in Q, V and N for the Cheng et al. experiments and N for the Shao et al. experiments.

The eddy diffusion coefficients from Cheng et al. [10] and Shao et al. [23] are plotted alongside the CFD derived diffusion coefficients (from the automated CFD study) in Fig. 9. The linear regression line from the CFD data, Equation (11), is also shown.

The experimental data in Fig. 9 sits close to, or just above, the linear regression line. The Cheng et al. [10] data generally follows the trend of the CFD data, the Shao et al. [23] data deviates further from the linear regression line as K increases. This supports the validity of the TKEB relationship with $L_{char} = \sqrt{A}$ (Equation (11)) but shows that for the set up used in the Shao et al. experiments, a steeper gradient may be more suitable. However, all the Shao et al. measured diffusion coefficients are, on average, within a factor of 2.0 of the values calculated by Equation (11). The Cheng et al. data is on average within a factor of 2.1 of the regression line. Therefore, despite the different type of ventilation, the relationship derived from the CFD data provides a useful method to estimate K in naturally ventilated spaces.

There may also be a case for using the TKEB relationship directly (i.e. Equation (9)). The gradient from the CFD data (0.824) is close to 1 and the CFD derived relationship under-predicts the two sets of experimentally derived coefficients.

It should be noted that Q, V and N for the experimental data could be different to the values chosen here and different values may affect the correlation of this data with the CFD derived model. It is also recognised that when applying the TKEB model, there may be some uncertainty

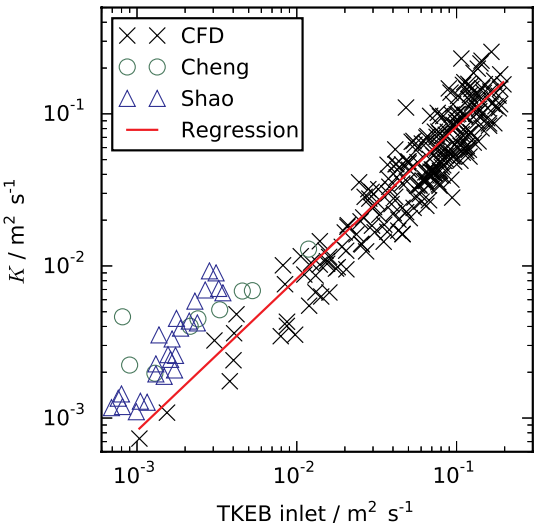

Fig. 9. K plotted against the TKEB relationship with $L_{char} = \sqrt{A}$. Data from the automated CFD models and from the experimental of Cheng et al. [10] and Shao et al. [23] are shown. The red line is Equation (11). (For interpretation of the references to colour in this figure legend, the reader is referred to the Web version of this article.)

over the values for Q, V and N in non-mechanically ventilated spaces.

3.3.2. Comparison with concentration time histories

An eddy diffusion model, with K calculated using the TKEB relationship, was used to predict gas concentrations in two scenarios, with the results compared to experimental data. The first scenario was the same meeting room experiment as used in the CFD validation in Section 2.2. Although this experiment was used to validate the CFD methodology, the room was not used in the automated CFD study. The second scenario was an assembly hall, see Fig. 10. The hall was approximately 1400 m^3 (maximum length, width and height of 29 m, 13 m, 5 m) and had a fresh air change rate, λ_f, of 3.8 h^{-1}, with no recirculation of air through the ventilation system. 14 slot type diffusers were located along the ceiling and the four extract grilles were on one wall. The supply vents directed the air straight down into the hall. A section of the hall (on the right in the schematic in Fig. 10) had a low ceiling and was poorly ventilated. It should be noted that more air was being extracted from the hall through the extract vents than was being supplied through the supply vents (3.8 h^{-1} vs. 2.0 h^{-1}). This means that air was also leaking into the room through other routes. For the purposes of the TKEB relationship, Q was set to the larger of the flow rates and N was set to the number of supply vents, as this is where bulk of the air entered the room.

In the assembly hall experiment the tracer gas, propylene, was released on one side of the room as shown in Fig. 10. 40 L of gas was released over approximately 20 s and the gas concentration was monitored using 20 UVICs, which were positioned at a range of heights across the room.

An eddy diffusion model was used to predict the tracer gas transport from the two experiments. Both experiments had a gas release with a constant rate, q, for a defined duration, t_{end}, so an eddy diffusion model was required which could represent this type of scenario. A model for a release with an infinite duration, was used by Cheng et al. [10] and Shao et al. [23]. This is reproduced below (Equation (13)) making the dependence on t explicit.

$$C_{cont}(t) = \int_0^t \frac{q \exp(-\lambda_f t)}{8(\pi K t)^{\frac{3}{2}}} r_x(t) r_y(t) r_z(t)\, dt, \tag{13}$$

where C_{cont} is the concentration from a continuous release. Using Equation (13) as the basis and taking advantage of the superposition principle for linear systems, a solution for the concentration due to a finite duration release, C_{finite}, has been produced in Equation (14).

$$C_{finite}(t) = \begin{cases} C_{cont}(t) & (t \le t_{end}) \\ C_{cont}(t) - C_{cont}(t - t_{end}) & (t > t_{end}) \end{cases} \tag{14}$$

The maximum, average and minimum concentrations for all monitoring locations are shown for both the eddy diffusion model and the experiments in Figs. 11 and 12. For the meeting room the maximum, average and minimum concentrations were taken from seven monitors, for the assembly hall it was 20.

Eddy diffusion models were run using K calculated from the linear regression line for the TKEB relationship (Equation (11)). Error metrics for the eddy diffusions models, calculated when the measured concentration was greater than 1 mg m^{-3}, are reported in Tables 3 and 4. It should be noted that error metrics were calculated from data at all the monitor locations, not just for the maximum, average and minimum data shown in Figs. 11 and 12. The geometric variance, VG, and geometric mean bias, MB, are reported along with the fraction of concentration predictions within a factor of two of the measurements, FAC2 [33], and the fraction of concentration predictions within a factor of five of the measurements, FAC5. A single-zone well-mixed model [2] was also built of both scenarios for comparison.

In both scenarios the eddy diffusion model performed reasonably well. In the meeting room, more than 80% of data points were within a factor of two of the experimental data. In the assembly hall, the model performance was lower, but still more than 88% of data points were within a factor of five of the experimental data. The lowest concentrations in the assembly hall were under-predicted quite significantly at early times. This has resulted in a large geometric variance.

According to the error metrics, a better fit was achieved for both scenarios by using the upper 95% PI equation to calculate K. The improved fit is also evident in the graph for the meeting room. In the assembly hall, however, the model's poor prediction of the lower concentrations has perhaps skewed the results when K was calculated using the linear regression equation. When using the upper 95% PI equation the lower concentration predictions have improved but the predictions for the higher concentrations (as illustrated by the maximum and average curves) are worse.

The faster mixing in the assembly hall compared to the that given by the linear regression line relationship (i.e. as illustrated by the under-prediction of the lower concentrations) may be due to the type of supply vents present. These were slot vents which directed the air down into the room, as opposed to the four-way diffusers in the automated study (from which the linear regression relationship was derived), which directed the air along the ceiling. This could mean that more of the turbulent kinetic energy generated at the inlet makes it into the lower parts of the room. In the meeting room experiment, the release was in the corner of the room so faster mixing would be expected (compared to the linear regression relationship), as discussed in Section 3.1.

The well-mixed model has performed well in comparison with the eddy diffusion models for both scenarios according to the error metrics. This is partly due to the type of tracer release used in both experiments. As a finite duration release was used in both scenarios the concentrations in the room tends towards a well-mixed condition with increasing time. However, it is clear in Figs. 11 and 12 how a well-mixed modelling approach is not suitable for predicting concentrations at early times.

3.4. Discussion

This comparison with the concentration time histories showed that the eddy diffusion model can perform well but the quality of the model is strongly dependent on the eddy diffusion coefficient, as would be expected. The TKEB relationship can be used to calculate the eddy

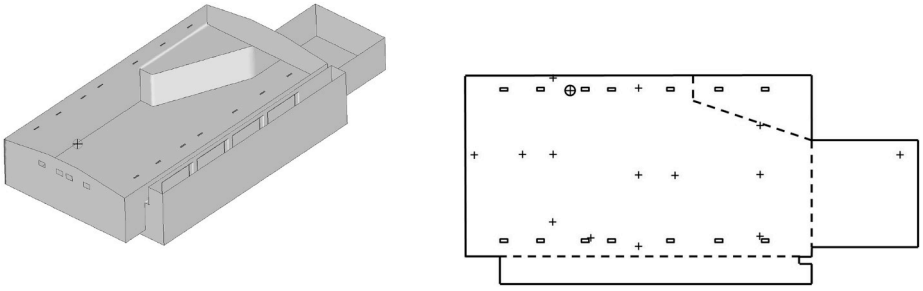

Fig. 10. A CAD drawing of the assembly hall (left). A schematic showing the layout used in the experiment (right). The open rectangles indicate the supply vents, the crosses indicate the UVIC locations and the circle with a cross shows the tracer gas release location. The dashed lines indicate different sections of the room.

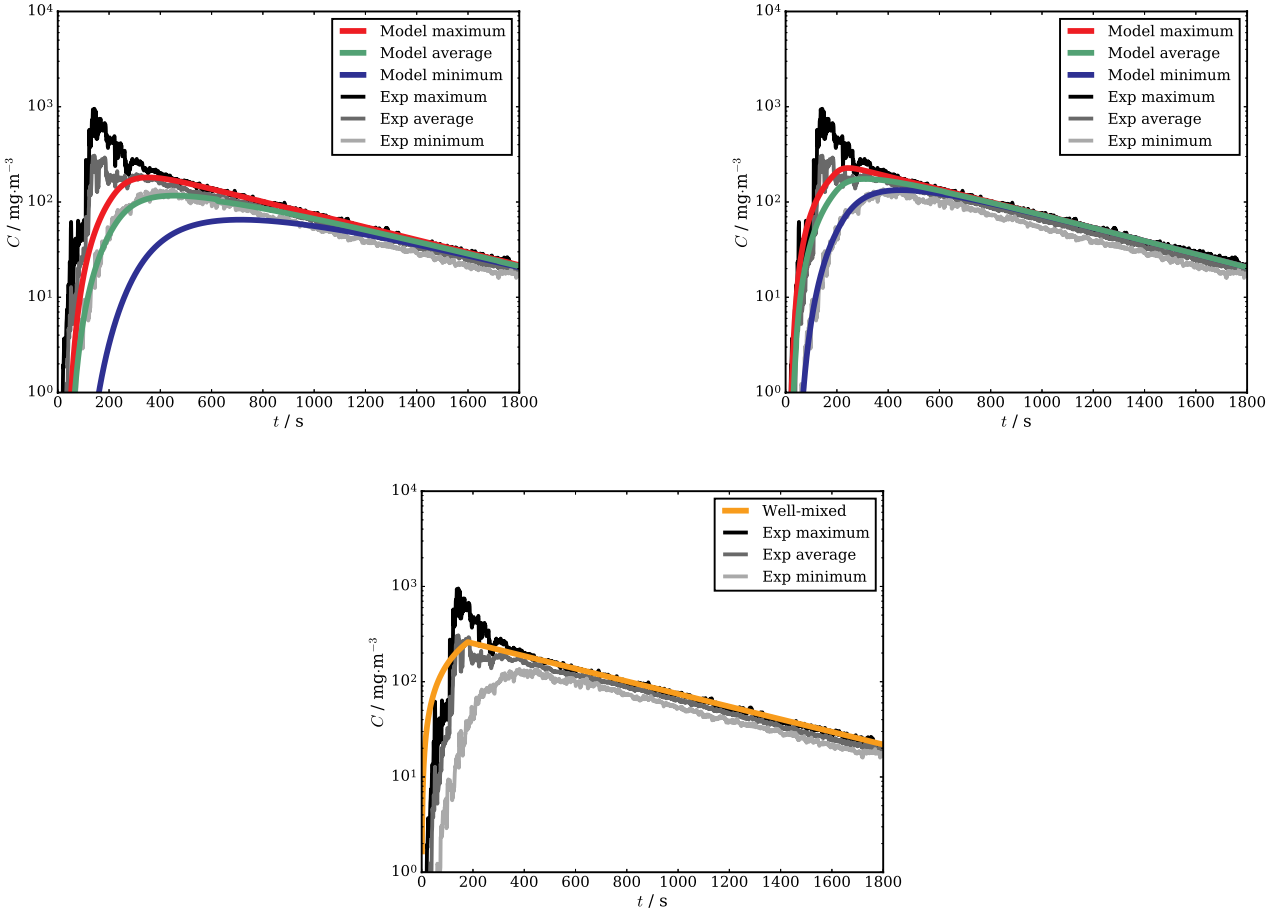

Fig. 11. Maximum, average and minimum tracer concentrations in the meeting room compared to predictions from an eddy diffusion model and a well-mixed model. Calculating K using the linear regression equation for the TKEB relationship, Equation (11) (upper left) and the upper 95% PI, Equation (10) (upper right). The results from a well-mixed model are shown (lower).

diffusion coefficient, but a small error in K can have a large effect on the lowest concentrations in the room.

An eddy diffusion model will have particular utility when there is a continuous release in a ventilated room. Under this condition a concentration gradient will always exist in the space so the difference between eddy diffusion and well-mixed approaches should be larger. This type of scenario can be relevant to the study of longer term exposure to toxic material or the transport of vapour from explosives for detection purposes.

Another scenario where eddy diffusion models will have merit over well-mixed models is when the user is interested in concentrations or exposures soon after an instantaneous or short duration release, before the room becomes mixed. This period is often of interest when considering health effects from an overt release of a toxic material, as people are likely to evacuate the space by later times. However, as discussed in Section 3.2, care should be taken when applying an eddy diffusion model close to the source at short times. This is because close to the source the concentration field will be more affected by local flow features, which eddy diffusion models are not designed to predict.

The comparisons with experimentally derived eddy diffusion coefficients show that the TKEB relationship has merit. The experimentally derived coefficients of Cheng et al. [10] and Shao et al. [23] follow the automated CFD data and linear regression line quite well.

If the scenario being studied is for an instantaneous or short duration release and the modeller is interested in concentrations or exposures at longer times or in smaller rooms then a well-mixed model may be sufficient. If the modeller is interested in what happens at very early times, or close to the source, then a more highly resolved model such as CFD may be required. For instantaneous and short duration releases, when the modeller is interested in what happens at intermediate times or in larger rooms, then an eddy diffusion model should give better results than a well-mixed model. The same is true for continuous releases in ventilated rooms. Models such as that by Drescher et al. [42] can be used to estimate when a room becomes well-mixed and to help guide when a particular model is required.

The validity of the TKEB relationship has been demonstrated using an automated CFD modelling approach. It should be noted that the scenarios studied consisted of only a small subset of possible indoor environments. The rooms were isothermal, had mixing ventilation, were cuboidal in shape and contained no furniture. However, through comparison with experimental data generated in other types of rooms, broader applicability of the relationship has been shown. Other features that have not been considered here include the mixing induced by movement of people or machinery and strong sources of buoyancy. It should also be noted that the eddy diffusion method in general is only applicable when there is isotropic mixing on a large scale due to laminar and/or turbulent motion.

It should be noted that first-order upwind schemes were used for discretisation of all scalar terms in the CFD and a first-order implicit scheme was used for the transient scalar transport to ensure convergence in the automated analysis. It is known that first-order schemes can cause numerical diffusion. However, when a sub-set of the models from the

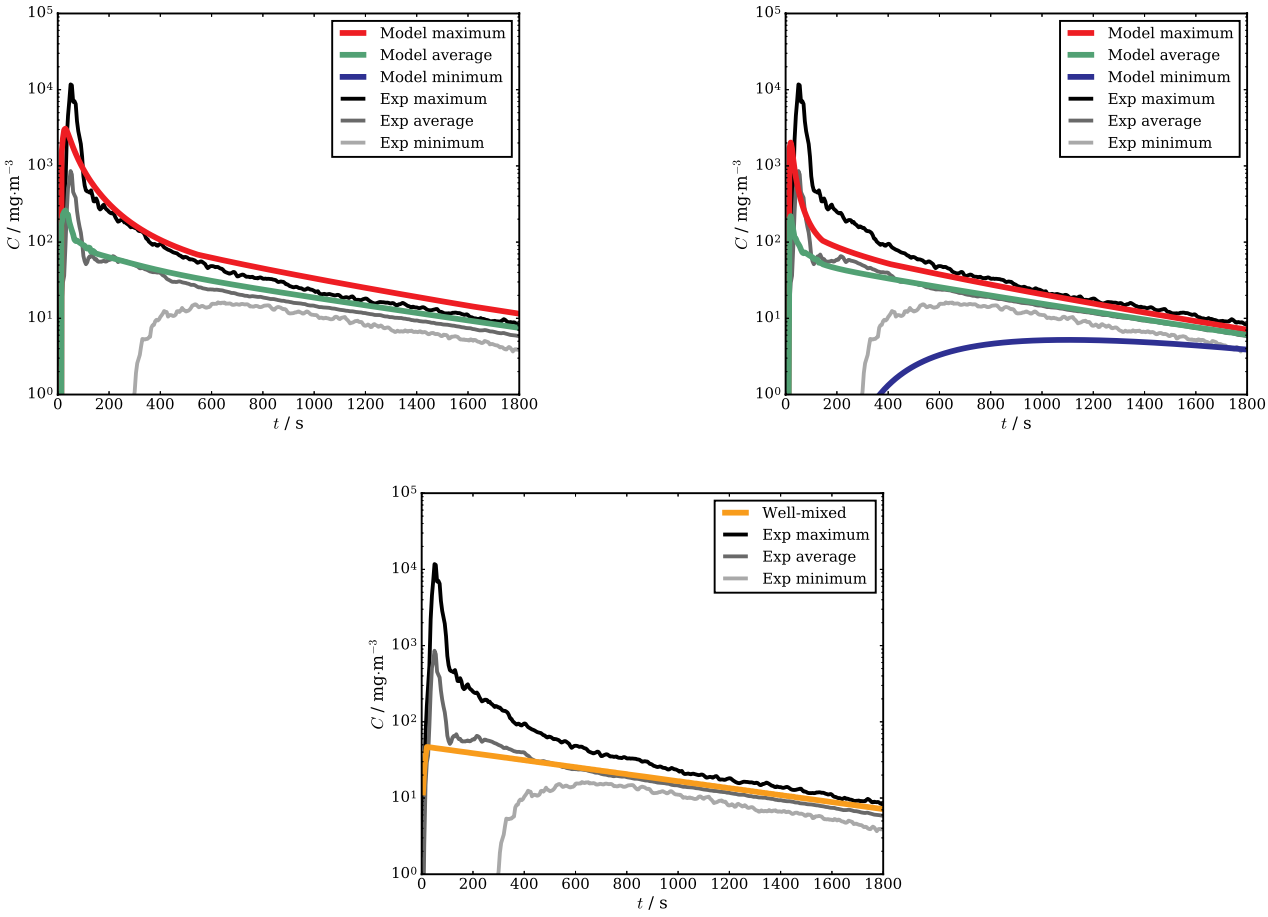

Fig. 12. Maximum, average and minimum tracer concentrations in the assembly hall compared to predictions from an eddy diffusion model and a well-mixed model. Calculating K using the linear regression line for the TKEB relationship, Equation (11) (upper left) and the upper 95% PI, Equation (10) (upper right). The results from a well-mixed model are shown (lower).

Table 3
Error metrics for eddy diffusion and well-mixed model concentration predictions compared to experimental data for the meeting room scenario. The first column gives the transport model used, the second gives the TKEB equation or method used to calculate K.

Model	TKEB eq.	K /m^2 s^{-1}	MB	VG	FAC2	FAC5
Eddy diffusion	Regression	0.033	1.50	4.10	0.80	0.90
Eddy diffusion	Upper PI	0.090	0.92	1.13	0.96	0.99
Well-mixed	–	–	0.73	1.64	0.89	0.95

Table 4
Error metrics for eddy diffusion and well-mixed model concentration predictions compared to experimental data for the assembly hall scenario. The first column gives the transport model used, the second gives the TKEB equation or method used to calculate K.

Model	TKEB eq.	K /m^2 s^{-1}	MB	VG	FAC2	FAC5
Eddy diffusion	Regression	0.019	1.49	6644	0.65	0.88
Eddy diffusion	Upper PI	0.076	0.99	1.79	0.88	0.96
Well-mixed	–	–	0.88	1.46	0.89	0.97

automated study were re-run using all second-order discretisation schemes, the fitted K values reduced by only a small amount, approximately 20% on average. Despite this effect being small, this additional uncertainty should be considered when interpreting the results of this study.

4. Conclusions

Fast running mathematical models of indoor dispersion have application in a number of areas. In particular, eddy diffusion models, where the rate of transport is governed by the eddy diffusion coefficient, K, can be used to rapidly predict spatially resolved concentrations. It has been shown that K can be predicted for isothermal room using the turbulent kinetic energy balance (TKEB) relationship which was originally proposed by Karlsson et al. [24]. The relationship had previously been applied using the room height as the characteristic length [9] but it has been demonstrated here that $\sqrt{A}$ is a more appropriate variable, which means that K is dependent on Q, V and N only.

An automated CFD approach was used to generate approximately 250 individual dispersion models which were then used to test the validity of the TKEB relationship and to calculate the constant for the relationship. It was shown that K was similar when calculated independently at three different heights. The release location did, however, have an effect on K. Releases occurring in the corner of the room, where the air flow is consistently faster, generally resulted in a higher K than releases which were away from the walls.

Eddy diffusion coefficients from two existing experimental data sets were compared to the coefficients derived from the CFD data and all data followed a similar trend. Using the TKEB relationship to calculate K, an eddy diffusion modelling approach was used to predict gas concentrations (from short duration releases) in two scenarios and predictions were compared to experimental data. In both cases the eddy diffusion model performed well but it was out-performed by a simple well-mixed model. However, this was due to the type of scenario considered and the time period examined.

The situations where an eddy diffusion model should have most merit over a well-mixed model are: for instantaneous and short duration releases, when the modeller is interested in what happens at intermediate times or in large rooms/spaces, and continuous releases in ventilated rooms when a concentration gradient will be maintained.

The TKEB relationship can be used to calculate K and the upper and lower 95% PI equations (or the lower K limit of 0.001 m^2s^{-1} [9]) can be used to understand the uncertainty. The TKEB relationship may not be suitable if the source imparts a large amount of energy to the room and, in the simplified form applied here, the relationship does not account for thermal effects.

Declaration of competing interest

The authors declare that they have no known competing financial interests or personal relationships that could have appeared to influence the work reported in this paper.

Acknowledgements

The research was supported by the United Kingdom Ministry of Defence. The authors would like to thanks Dr Zheng-Tong Xie of Southampton University for his support and feedback regarding the TKEB relationship. Timothy Foat would also like to acknowledge the support of the PhD scheme in the Faculty of Engineering and Physical Sciences at the University of Southampton.

Appendix A. Supplementary data

Supplementary data related to this article can be found at https://doi.org/10.1016/j.buildenv.2019.106591.

References

[1] C. Keil, C. Simmons, T. Anthony, Mathematical Models for Estimating Occupational Exposure to Chemicals, American Industrial Hygiene Association, 2009.
[2] P. Reinke, C. Keil, Well-mixed box models, in: C.B. Kiel, C.E. Simmons, T. R. Anthony (Eds.), Mathematical Models for Estimating Occupational Exposure to Chemicals, American Industrial Hygiene Association, 2009, pp. 23–31. Ch. 4.
[3] M. Nicas, Estimating exposure intensity in an imperfectly mixed room, Am. Ind. Hyg. Assoc. J. 57 (6) (1996) 542–550.
[4] C. Feigley, J. Bennett, E. Lee, J. Khan, Improving the use of mixing factors for dilution ventilation design, Appl. Occup. Environ. Hyg 17 (5) (2002) 333–343.
[5] A. Megri, F. Haghighat, Zonal modeling for simulating indoor environment of buildings: review, recent developments, and applications, HVAC R Res. 13 (6) (2007) 887–905.
[6] M. Nicas, Modeling turbulent diffusion and advection of indoor air contaminants by Markov chains, Am. Ind. Hyg. Assoc. J. 62 (2) (2001) 149–158.
[7] M. Nicas, Turbulent eddy diffusion models, in: C.B. Kiel, C.E. Simmons, T. R. Anthony (Eds.), Mathematical Models for Estimating Occupational Exposure to Chemicals, American Industrial Hygiene Association, 2009, pp. 53–65. Ch. 7.
[8] A. Nehorai, Detection and localization of vapour-emitting sources, IEEE Trans. Signal Process. 43 (1) (1995) 243–253.
[9] P. Drivas, P. Valberg, B. Murphy, R. Wilson, Modeling indoor air exposure from short-term point source releases, Indoor Air 6 (1996) 271–277.
[10] K.-C. Cheng, V. Acevedo-Bolton, R.-T. Jiang, N. Klepeis, W. Ott, O. Fringer, L. Hildemann, Modeling exposure close to air pollution sources in naturally ventilated residences: Association of turbulent diffusion coefficient with air change rate, Environ. Sci. Technol. 45 (9) (2011) 4016–4022.
[11] W. Zhu, Q. Chen, Real-time or faster-than-real-time simulation of airflow in buildings, Indoor Air 19 (2009) 33–44.
[12] W. Zuo, Q. Chen, Fast and informative flow simulations in a building by using fast fluid dynamics model on graphics processing unit, Build. Environ. 45 (3) (2010) 747–757.
[13] B. Elhadidi, H. Khalifa, Comparison of coarse grid lattice Boltzmann and Navier Stokes for real time flow simulations in rooms, Build. Simul. 6 (2) (2013) 183–194.
[14] M. Khan, N. Delbosc, C. Noakes, J. Summers, Real-time flow simulation of indoor environments using lattice Boltzmann method, Build. Simul. 8 (4) (2015) 405–414.
[15] Crank, Mathematics of Diffusion, Oxford University Press, UK, 1979.
[16] P. Scheff, R. Friedman, J. Franke, L. Conroy, R. Wadden, Source activity modeling of freon emissions from open-top vapor degreasers, Appl. Occup. Hyg. 7 (2) (1992) 127–134.
[17] W. Shade, M. Jayjock, Monte Carlo uncertainty analysis of a diffusion model for the assessment of halogen gas exposure during dosing of brominators, Am. Ind. Hyg. Assoc. J. 58 (6) (1997) 418–424.
[18] E. Donovan, B. Donovan, J. Sahmel, P. Scott, D. Paustenbach, Evaluation of bystander exposures to asbestos in occupational settings: a review of the literature and application of a simple eddy diffusion model, Crit. Rev. Toxicol. 41 (1) (2011) 50–72.
[19] T. Zontek, S. Hollenbeck, J. Jankovic, B. Ogle, Modeling particle emissions from three-dimensional printing with acrylonitrile-butadiene-styrene polymer filament, Environ. Sci. Technol. 53 (16) (2019) 9656–9663.
[20] D. Drolet, T. Armstrong, Ih mod 2.0. ms excel workbook of deterministic and Monte Carlo simulation mathematical models to estimate airborne concentrations of chemicals. https://www.aiha.org/public-resources/consumer-resources/topics-of-interest/ih-apps-tools accessed: 30/09/19 (2018).
[21] T. Foat, S. Parker, I. Castro, Z.-T. Xie, Numerical investigation into the structure of scalar plumes in a simple room, J. Wind Eng. Ind. Aerodyn. 175 (2018) 252–263.
[22] D. Cooper, M. Horowitz, Exposures from indoor powder release: models and experiments, Am. Ind. Hyg. Assoc. J. 47 (4) (1986) 214–218.
[23] Y. Shao, S. Ramachandran, S. Arnold, G. Ramachandran, Turbulent eddy diffusion models in exposure assessment-determination of the eddy diffusion coefficient, J. Occup. Environ. Hyg. 14 (3) (2017) 195–206.
[24] E. Karlsson, A. Sjöstedt, S. Håkansson, Can weak turbulence give high concentrations of carbon dioxide in baby cribs? Atmos. Environ. 28 (7) (1994) 1297–1300.
[25] M. Jayjock, C. Chaisson, S. Arnold, E. Dederick, Modeling framework for human exposure assessment, J. Expo. Sci. Environ. Epidemiol. 17 (2007) S81–S89.
[26] T. Foat, J. Nally, S. Parker, Investigating a selection of mixing times for transient pollutants in mechanically ventilated, isothermal rooms using automated computational fluid dynamics analysis, Build. Environ. 118 (2017) 313–322.
[27] J. Srebric, Q. Chen, Simplified numerical models for complex air supply diffusers, HVAC R Res. 8 (3) (2002) 277–294.
[28] ARID, UVIC MkII User's Manual, ARID Ltd, 2004.
[29] ICON, IconCFD 3.3 Technical User Guide, 2017.
[30] S. Patankar, D. Spalding, A calculation procedure for heat, mass and momentum transfer in three-dimensional parabolic flows, Int. J. Heat Mass Transf. 15.
[31] B. Van Leer, Towards the ultimate conservative difference scheme. v. a second-order sequel to godunov's method, J. Comput. Phys. 32 (1) (1979) 101–136.
[32] H. Wang, Z. Zhai, Application of coarse-grid computational fluid dynamics on indoor environment modeling: optimizing the trade-off between grid resolution and simulation accuracy, HVAC R Res. 18 (5) (2012) 915–933.
[33] S. Hanna, O. Hansen, S. Dharmavaram, FLACS CFD air quality model performance evaluation with Kit Fox, MUST, Prairie Grass, and EMU observations, Atmos. Environ. 38 (28) (2004) 4675–4687.
[34] I. Sobol, Distribution of points in a cube and approximate evaluation of integrals, USSR Comput. Math. Math. Phys. 7 (1967) 86–112.
[35] Trox, Ceiling diffusers type ADT. https://www.troxuk.co.uk/ceiling-diffusers/type-adt-995f6e2818a938ff accessed: 25/07/18 (2018).
[36] H. Awbi, Ventilation of Buildings, Spon Press, New York, 2003.
[37] ASHRAE, Handbook of Fundamentals, American Society of Heating, Refrigeration and Air-Conditioning Engineers, Atlanta, GA, 2001.
[38] R. Byrd, P. Lu, J. Nocedal, C. Zhu, A limited memory algorithm for bound constrained optimization, SIAM J. Sci. Comput. 16 (5) (1995) 1190–1208.
[39] Y. Tominaga, T. Stathopoulos, Turbulent schmidt numbers for CFD analysis with various types of flowfield, Atmos. Environ. 41 (2007) 8091–8099.
[40] T. van Hooff, B. Blocken, P. Gousseau, G. van Heijst, Counter-gradient diffusion in a slot-ventilated enclosure assessed by LES and RANS, Comput, Fluid 96 (2014) 63–75.
[41] J. Eisenhauer, Regression through the origin, teach, Stat 25 (3) (2003) 76–80.
[42] A. Drescher, C. Lobascio, A. Gadgil, W. Nazaroff, Mixing of a point-source indoor pollutant by forced convection, Indoor Air 5 (3) (1995) 204–214.